Available online at www.sciencedirect.com
ScienceDirect
International Journal of Heat and Mass Transfer 51 (2008) 3985–4001
International Journal of HEAT and MASS TRANSFER
www.elsevier.com/locate/ijhmt

Second law analysis of a disturbed flow in a thin slit with wall suction or injection

Fethi Kamışlı

Department of Chemical Engineering, Firat University, 23119 Elazig, Turkey

Received 16 May 2007; received in revised form 14 September 2007
Available online 31 January 2008

Abstract

Fully-developed laminar flow in a horizontal thin slit having plates at different temperature is considered for the case of lower plate movement and/or the pressure gradient-and-upper plate movement. The flow under these conditions is analyzed in terms of entropy generations as function of the Prandtl number, the Eckert number, cross-flow Reynolds number and dimensionless temperature difference. In this context, the governing equations for distributions of temperature, the dimensionless entropy generation number and Bejan number are analytically derived with the aid of expressions for velocity distributions. The effect of each parameter on the temperature and the entropy generation are investigated by varying one of the parameters and keeping the rest of them constant for each flow case. The effects of viscous dissipation, rates of mass suction/injection and dimensionless temperature differences on the fluid temperature and entropy generation are examined. The magnitudes of mass suction and/or injection have a large influence on the temperature profile of the fluid. It is observed that the Prandtl number and the Eckert number affect fluid temperature in similar way. It is found that an increase in values of the cross-flow Reynolds number (mass suction/injection) enhances the entropy generation in boundary layer. The velocity profiles are found to be in agreement with the distributions of the dimensionless entropy generation number (N_S) for two flow cases.

Keywords: Second law analysis; Entropy generation; Wall suction/injection

1. Introduction

Low Reynolds number flow and heat transfer in a porous medium has long been an important subject in the field of chemical, biochemical, and environmental science. Along with the advancement of science and technology, modern instruments and equipment such as micro-electro-mechanical systems, laser coolant lines and compact heat exchangers are being used for many purposes. Laminar heating and cooling occur in increasing variety in such instruments.

There is an increased need for conserving useful energy and thus, producing thermodynamically efficient heat transfer processes in which internal forced convection heat transfer occurs. The foundation of knowledge of entropy generation goes back to Clausius and Kelvin's studies on the irreversible aspects of the second law of thermodynamics. Fluid flow through porous media is of fundamental interest and is of great practical importance in many diverse applications, including the production of oil and gas from geological structures, the gasification of coal, the retorting of shale oil, filtration, ground-water movement, regenerative heat exchange, surface catalysis of chemical reactions, adsorption, coalescence, drying, ion exchange and chromatography.

As expressed previously, the flow of fluid through porous media and in channels of circular or rectangular cross-section with the porous walls has long been investigated in many engineering applications. Wang et al. [1] theoretically investigated flow distribution and pressure drop in a channel with a porous wall. An analytical solution of the non-linear ordinary differential equations, based on the varying flow coefficients, was obtained. They claimed

E-mail address: fkamisli@firat.edu.tr

0017-9310/$ - see front matter © 2007 Elsevier Ltd. All rights reserved.
doi:10.1016/j.ijheatmasstransfer.2007.10.038

Nomenclature

A	constant
B	constant
Be	Bejan number, $1/(1+\phi)$
Br	Brinkman number, $EcPr$
C_P	specific heat, J kg^{-1} K^{-1}
Ec	Eckert number, $u_m^2/C_p\Delta T$
k	thermal conductivity, W m^{-1} K^{-1}
v_x	dimensionless axial velocity, $\tilde{v}_x/u_m$
u_m	axial average velocity, m s^{-1}
$\tilde{v}_x$	axial velocity, m s^{-1}
V	transverse direction, m s^{-1}
$\tilde{x}$	axial direction
$\tilde{y}$	transverse direction
h	transverse direction between plates, m
y	dimensionless transverse direction
x	dimensionless axial direction
N_X	entropy generation number, conduction $= (\partial\theta/\partial x)^2/Pe^2$
N_F	entropy generation number, fluid friction, $Br(\partial v_x/\partial y)^2/\Omega$
N_S	entropy generation number, total
N_Y	entropy generation number, normal to the axis $= (\partial\theta/\partial y)^2$
p	positive integer $= 1, 2, 3, \ldots, \infty$
P	dimensionless pressure
P_0	dimensionless pressure gradient, dP/dx
Pe	Peclect number, $\rho C_p u_m h/k$
Pr	Prandtl number, $\mu C_p/k$
Re	cross-flow Reynolds number, $\rho V h/\mu$
S_G	entropy generation rate, W m^{-3} K^{-1}
$S_{G,C}$	characteristic entropy transfer rate
t	dimensionless time
T	temperature, K
T_1	reference temperature, K
T_2	reference temperature at the upper plate, K

Greek symbols

θ	dimensionless temperature
Ω	dimensionless temperature difference, $\Delta T/T_1$
ϕ	irreversibility ratio, $N_F/(N_X+N_Y)$
μ	dynamic viscosity, Pa s
ρ	density of the fluid, kg m^{-3}

that the predicted flow distribution agrees well with experimental data. Hayat et al. [2] studied the flow of a third-order fluid occupying the space over a porous wall. The suction or blowing velocity was applied at the surface of the wall. By introducing a velocity field, the governing equations are reduced to a non-linear partial differential equation and the resulting equation was analytically solved by using Lie group methods. Fang [3] undertook an analysis of an unsteady laminar flow of a Newtonian fluid confined in a tube of rectangular cross-section with porous wall. The steady state temperature distributions were also presented. It was concluded that the transient velocity and mass transfer across the fluid have great influence on the velocity and temperature distributions that affects the heat transfer behavior at the two plates. In another paper [4] Fang obtained analytically the unsteady velocity profiles for a pressure-driven Poiseuille flow in a channel with porous walls under mass transfer. He discussed the influences of mass transfer on transient velocity and steady state temperature profiles.

Deng and Martinez [5] studied the viscous flow of a Newtonian fluid in a channel partially filled with a porous medium and having a porous wall. In the porous medium the Brinkman–Darcy law relationship was considered. In order to solve model equations, a similarity variable was used to reduce the governing equations to two coupled, non-linear ordinary differential equations.

Ariel [6] obtained the exact analytical solutions of two problems of laminar flow of a second-order fluid confined in a tube of rectangular cross-section and annulus with porous walls. For each problem the rate of injection at one wall is assumed to equal to the rate of suction at the other wall. It was reported that the viscoelasticity of the fluid tends to destroy the formation of the boundary layer at the wall where the suction takes place for large values of the cross-flow Reynolds number.

Zaturska and Banks [7] analyzed the flow of a Newtonian fluid in a tube of rectangular cross-section. They reported that an exact solution of the simplified Navier–Stokes equation for the certain conditions decays with increasing time if the Reynolds number is less than a critical value and grows without limit if Reynolds number is larger than that critical value.

Ogulu and Amos [8] worked on the problem of suction/injection on free convective flow of a non-Newtonian fluid past a vertical porous plate. The non-linear partial differential equations are decoupled. Expressions for temperature, velocity, skin-friction and rate of heat transfer were obtained at very slow motion of incompressible fluid. They observed that the velocity distribution is highly dependent on the viscoelastic parameter and the rate of heat transfer does not depend on the free convective parameter.

Bejan [9] performed an analytical study to show entropy generation in fundamental convective heat transfer problems such as pipe flow, boundary layer over flat plate, single cylinder in cross-flow, flow in the entrance region of a flat rectangular duct. He demonstrated that how the flow geometric parameters may be selected in order to minimize the irreversibility associated with a specific convective heat transfer process. Nag and Mukherjee [10] investigated the thermodynamic optimization for convective heat transfer through a duct with constant wall temperature. They indi-

cated that initial temperature difference between the fluid and the wall is an important design criterion and there is an optimum ratio of the heat transfer to pumping power ratio. Entropy generation in a vertical concentric channel was studied analytically by Tasnim and Mahmud [11]. They took into account temperature dependent viscosity for laminar flow. Finally, they derived analytical expressions for the velocity and temperature to obtain expressions for local and average entropy generation for that geometry. Similarly, entropy generation with variable viscosity was analyzed by Sahin [12] for laminar duct flow. The shape of the duct on entropy generation was also studied by Sahin [13]. He compared the circular, square, triangular, rectangular and sinusoidal cross-sectional duct from the entropy generation point of view. Recently, Mahmud and Fraser [14] investigated the entropy generation for laminar flow of a Newtonian fluid confined in different geometries. In another paper [15] Mahmud and Fraser worked on the second law analysis of fluid flow and heat transfer inside a circular duct under fully developed forced convection for non-Newtonian fluids. The governing equations were solved numerically in order to obtain Nusselt number for some selected fluid indices. Naphon [16] theoretically and experimentally studied the second law analysis of the heat transfer and flow in a horizontal concentric tube heat exchanger. He developed the mathematical model based on the conservation equations of energy and solved this equation numerically by the central finite difference method to obtain temperature distributions, entropy generation, and exergy loss. It was reported that there is reasonable agreement between predicted results and measured data. On the other hand, Guo et al. [17] performed theoretical analysis and experimental confirmation for the principle to improve thermal performance of heat exchangers. The uniformity of the temperature difference field (TDF) and effectiveness of various types of heat exchangers were studied analytically and numerically. It was reported that the analysis of entropy generation caused by the heat transfer indicates that the uniformity principle of TDF satisfies the second law of thermodynamics. It was also observed that the experimental results governed by the uniformity principle of TDF show that the effectiveness increases with the increase of the uniformity of TDF.

Since conserving useful energy and thus, producing thermodynamically efficient heat transfer processes are quite important in energy saving, reducing the process irreversibility is the most common desire in many engineering implications. In this context, many convective heat transfer processes have been analyzed in terms of entropy generations as mentioned earlier. To the author's knowledge; however, to date none of the previous studies has dealt with the second law analysis of an incompressible fluid that is disturbed by either mass suction or injection, for flow in a thin slit having porous walls at different temperature. Therefore, the main purpose in the present study is to analyze the entropy generation due to heat conduction in the transverse direction and the viscous dissipation for (1) the lower plate movement and (2) the pressure gradient-and-upper plate movement. In this context, the governing equations for velocities of plate movement-driven flow and pressure-and-plate movement-driven flow are used to obtain analytical expressions for the fluid temperature and thus the entropy generation distributions as functions of the Prandtl number, the Eckert number and the dimensionless temperature difference for the cases of mass injection and suction at the bottom plate.

2. The derivation of basic equations and theoretical analysis

Consider an incompressible fluid flowing in x-direction in a horizontal slit (two parallel plates) with porous walls at different temperatures, with mass injection through one plate and the same amount of mass suction through other (see Fig. 1). Two flow problems are considered namely (1) the lower plate undergoes a sudden acceleration with a constant velocity of u_m and (2) an imposed pressure drop and the upper plate movement that undergoes a sudden acceleration to a constant velocity of u_m.

At unsteady state the governing equations for velocity of a power-law fluid for both cases were obtained by taking $n = 1$ in the power-law fluid model at various values of Reynolds number to examine the effect of mass suction/injection on velocity profiles. The effect of mass suction/injection, the power-law index and the time on the velocity profiles were examined in elsewhere [18,19]. Therefore, the derivations of the velocity profiles for both cases are not repeated here. However, the governing equations for heat transfer at steady state will be given in order to obtain temperature profiles and thus entropy generation profiles as functions of the Prandtl number, the Eckert number and the dimensionless temperature difference for the cases of mass suction or injection.

While in the previous papers [18,19] the unsteady state flows in a slit with porous plates were analyzed as functions of time and cross-flow rates at the bottom plate for two different flow cases. Here, the equations for temperature and entropy distributions of the flow in a thin horizontal slit are analytically derived with the aid of the previously developed velocity equations in order to perform the second law analysis for the problem at hand. In the present paper,

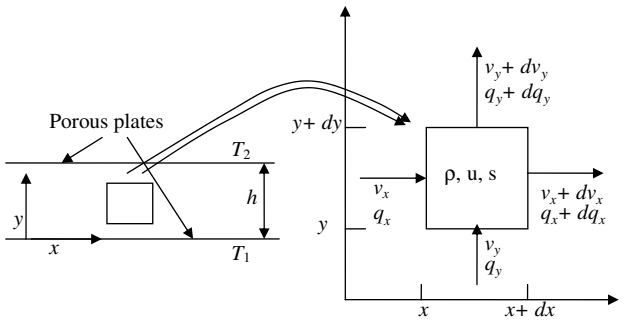

Fig. 1. Schematic diagram of entropy generation analysis for an infinitesimal fluid element $dx \times dy$ in two large parallel porous plates.

a Newtonian fluid flow disturbed by cross-flow at the bottom plate the entropy generation due to irreversibility of process is examined in the thin horizontal slit whose walls are at different temperatures.

The focus is on the development of heat transfer equation, with the aid of the developed velocity distribution for the flow cases. The resulting expression will be used for numerically computing temperature and entropy generation distributions as a function of the Prandtl number, the Eckert number and the dimensionless temperature difference for the cases of mass suction/injection.

It is desirable to analyze the system in terms of distributions of velocity, momentum flux, temperature and entropy generation at a constant wall heat flux or a constant wall temperature.

At unsteady state the velocities for the lower plate movement-driven flow [18] and the pressure-and-upper plate movement-driven flow [19] were given by following equations, respectively:

$$v_x(t,y) = \frac{\exp(Rey) - \exp(Re)}{1-\exp(Re)} - 2\pi \exp(-Re^2 t/4)\exp(Rey/2) \times \sum_{p=1}^{\infty} \frac{p\sin(p\pi y)}{p^2\pi^2 + Re^2/4}\exp(-p^2\pi^2 t) \tag{1a}$$

The above equation is obtained subject to boundary conditions:

$$v_x(t,0) = 1, \quad v_x(t,1) = 0 \quad \text{and} \quad v_x(0,y) = 0$$

$$v_x(t,y) = -\frac{P_0}{Re}y + \frac{(P_0+Re)}{Re}\left(\frac{1-\exp(Rey)}{1-\exp(Re)}\right) + \exp(-Re^2 t/4) \times \sum_{p=1}^{\infty} \frac{\sin(p\pi y)}{p^2\pi^2 + Re^2/4} \times \exp(-p^2\pi^2 t)\left\{\sin(p\pi y)\left[-P_0 y - \frac{2P_0(Re^2/4-(p\pi)^2)}{Re(Re^2/4+(p\pi)^2)} + (P_0+Re)\left(\frac{1+\exp(Rey)}{1-\exp(Re)}\right)\right] + (p\pi)\cos(p\pi y)\left[-\frac{2P_0}{Re}y - \frac{P_0}{(Re^2/4+(p\pi)^2)} + \frac{2(P_0+Re)}{Re}\left(\frac{1-\exp(Rey)}{1-\exp(Re)}\right)\right]\right\} \tag{1b}$$

The above equation is also derived subject to boundary conditions:

$$v_x(t,0) = 0, \quad v_x(t,1) = 1 \quad \text{and} \quad v_x(0,y) = 0$$

where Re is the cross-flow Reynolds number, P_0 the dimensionless pressure gradient in the axial direction, $v_x(t,y)$ the unsteady state dimensionless velocity in the axial direction and the dimensionless variables appeared in the above equations are given as follows (for details see [19]):

$$x = \tilde{x}/\ell, \quad v_x = \tilde{v}_x/u_m, \quad t = \tilde{t}/(h^2\rho/\mu), \quad P = \tilde{P}/(\mu u_m/\ell)$$

where ℓ is the axial distance. The dimensionless transient velocity profiles as a function of the dimensionless transverse distance are obtained by use of Eq. (1b) and graphically illustrated in Fig. 2 at certain values of Reynolds number and dimensionless time for various values of dimensionless pressure gradient. The dimensionless time taken to be 0.14 in present computation is large enough for the dimensionless transient velocity to be considered like steady state velocity (see [19]).

It is difficult to solve exactly the transient energy equations with viscous dissipation by using these transient velocity expressions. Since the flow will be developed after a certain time, it is of practical use to solve the steady state energy equation. Therefore, in the above equations the steady state parts of the velocity will be taken for evaluating viscous dissipation in the development of the steady state energy equation for each flow case.

The steady state velocity for the lower plate movement-driven flow and the pressure-and-upper plate movement-driven flow are respectively given as follow:

$$v_x(y) = \frac{\exp(Re) - \exp(Rey)}{\exp(Re)-1} \tag{2a}$$

$$v_x(y) = -\frac{P_0}{Re}y + \frac{(P_0+Re)}{Re}\left(\frac{\exp(Rey)-1}{\exp(Re)-1}\right) \tag{2b}$$

As stated previously the incompressible viscous fluid with constant physical properties of ρ, μ, k, C_p is flowing in the laminar flow regime in a slit of height h. For $x > 0$ there are constant wall temperatures specifically T_1 and T_2 for the bottom plate and the upper plate respectively. The dimensionless velocity distributions, at least far enough downstream from the inlet so that the entrance length has been exceeded, can be computed from the equations just given above.

In order to obtain the temperature distribution, the following partial differential equation has to be solved with the appropriate boundary conditions.

$$\rho C_p u_m \frac{\partial T}{\partial \tilde{y}} = k\left[\frac{\partial^2 T}{\partial \tilde{y}^2}\right] + \mu\left(\frac{\partial \tilde{v}_x}{\partial \tilde{y}}\right)^2 \tag{3}$$

where u_m is the velocity of mass either injection or suction (cross-flow velocity) at the bottom plate. In order to obtain the above equation in the dimensionless form, the dimensionless variables are defined as follows:

$$v_x = \tilde{v}_x/u_m, \quad y = \tilde{y}/h \quad \text{and} \quad \theta = (T-T_1)/(T_2-T_1)$$

By utilizing the above dimensionless variables the energy equation is rewritten in dimensionless form as follows:

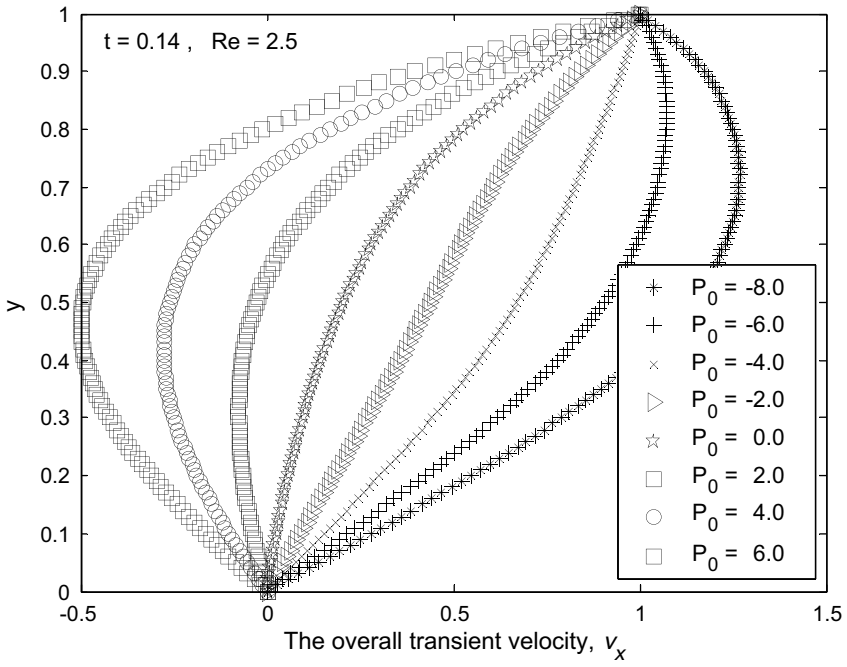

Fig. 2. The overall transient velocity distribution for various values of pressure drop at constant values of dimensionless time and cross-flow Reynolds number.

$$\frac{\partial^2\theta}{\partial y^2} - RePr\frac{\partial\theta}{\partial y} = -EcPr\left(\frac{\partial v_x}{\partial y}\right)^2 \tag{4}$$

In order to obtain temperature profiles for each flow case, the above equation has to be solved subject to the boundary conditions:

$$\theta = 0 \quad \text{at } y = 0 \quad \text{and} \quad \theta = 1 \quad \text{at } y = 1 \tag{5}$$

where θ is the dimensionless temperature defined above. After the fluid is far downstream from the beginning of the entrance, one expects intuitively that the constant wall temperature will result in the constant fluid temperature in the axial direction. One further expects that the shape of the transverse temperature profiles will ultimately not undergo further change with increasing x.

Substituting the derivative of Eq. (2a) with respect to y into Eq. (4) gives the following equation:

$$\frac{\partial^2\theta}{\partial y^2} - RePr\frac{\partial\theta}{\partial y} = -EcPr\frac{Re^2 e^{2Rey}}{(e^{Re}-1)^2} \tag{6}$$

The governing equation (6) for the temperature distribution of the lower plate movement-driven flow can be easily solved subject to boundary condition given by Eq. (5) and the solution of this equation is given by

$$\theta = \frac{e^{RePry}-1}{e^{RePr}-1} + \frac{e^{RePry}-1}{e^{RePr}-1}\left[\frac{EcPr(e^{2Re}-1)}{2(2-Pr)(e^{Re}-1)^2}\right] - \frac{EcPr(e^{2Rey}-1)}{2(2-Pr)(e^{Re}-1)^2} \tag{7}$$

It is obvious that the first terms in Eq. (7) is the solution of energy equation when viscous dissipation term is ignored in Eq. (4), and the second and third terms result from viscous dissipation of the fluid by the lower plate movement. As can be seen from Eq. (7) the temperature distribution is linearly dependent on the Eckert number. It is seen that when either $Re = 0$ or $Pr = 2$ in Eq. (7), the dimensionless temperature goes to infinity, an unrealistic value. As $Re = 0$, the problem becomes the well-known Couette flow and the temperature distribution was given in [22]. On the other hand, the solution of energy equation, valid for $Pr = 2$, has to be determined for the lower plat movement-driven flow. The solution is given as follows:

$$\theta = \frac{e^{2Rey}-1}{e^{2Re}-1} + \frac{e^{2Rey}-1}{e^{2Re}-1}\left[\frac{EcRee^{2Re}}{2(e^{Re}-1)^2}\right] - \frac{EcRe}{2(e^{Re}-1)^2}ye^{2Rey} \tag{8}$$

As stated earlier, it was assumed that the flow is laminar and fully developed. Therefore, the boundary layers are no longer growing thicker and it is expected that h_0 (the mean heat transfer coefficient) on the plates will become constant and thus the temperature profiles will retain the same shape along the axial direction.

Substituting the derivative of Eq. (2b) with respect to y into Eq. (4) gives the following equation:

$$\frac{\partial^2\theta}{\partial y^2} - RePr\frac{\partial\theta}{\partial y} = -EcPr\left(\frac{(Re+P_0)^2e^{2Rey}}{(e^{Re}-1)^2} - 2\frac{(Re+P_0)}{Re(e^{Re}-1)}e^{Rey} + \left(\frac{P_0}{Re}\right)^2\right) \tag{9}$$

where $P_0 = dP/dx$ is the dimensionless pressure gradient in the axial direction. The governing equation (9) for the

temperature distribution of the pressure-and-upper plate movement-driven flow can be analytically solved and its general solution is given by

$$\theta = A + B\mathrm{e}^{RePry} + \frac{EcPrP_0^2}{PrRe^3}y + \frac{2EcPr(P_0+Re)P_0}{Re^3(1-Pr)(\mathrm{e}^{Re}-1)}\mathrm{e}^{Rey} - \frac{EcPr(P_0+Re)^2}{2Re^2(1-Pr)(\mathrm{e}^{Re}-1)^2}\mathrm{e}^{2Rey} \quad (10)$$

In the above equation A and B are the integration constants that are determined by applying boundary conditions given by Eq. (5) as follows:

$$A = -\frac{1}{(\mathrm{e}^{PrRe}-1)}\left[1 - \frac{2EcPrP_0(P_0+Re)}{Re^3(1-Pr)} + \frac{EcPr(P_0+Re)^2(\mathrm{e}^{2Re}-1)}{2Re^2(2-Pr)(\mathrm{e}^{Re}-1)^2} - \frac{EcPrP_0^2}{PrRe^3}\right] - \frac{2EcPrP_0(P_0+Re)}{Re^3(1-Pr)(\mathrm{e}^{Re}-1)} + \frac{EcPr(P_0+Re)^2}{2Re^2(2-Pr)(\mathrm{e}^{Re}-1)^2}$$

$$B = \frac{1}{(\mathrm{e}^{PrRe}-1)}\left[1 - \frac{2EcPrP_0(P_0+Re)}{Re^3(1-Pr)} + \frac{EcPr(P_0+Re)^2(\mathrm{e}^{2Re}-1)}{2Re^2(2-Pr)(\mathrm{e}^{Re}-1)^2} - \frac{EcPrP_0^2}{PrRe^3}\right]$$

Substituting the integration constants (A and B) into Eq. (10) results in the solution of energy equation for the pressure-and-upper plate movement-driven flow in the following form:

$$\theta = \frac{\mathrm{e}^{RePry}-1}{(\mathrm{e}^{PrRe}-1)} + \frac{EcPr}{Re^2}\left\{\frac{\mathrm{e}^{RePry}-1}{(\mathrm{e}^{PrRe}-1)} \times \left[-\frac{2P_0(P_0+Re)}{Re(1-Pr)} + \frac{(P_0+Re)^2(\mathrm{e}^{2Re}-1)}{2(2-Pr)(\mathrm{e}^{Re}-1)^2} - \frac{P_0^2}{PrRe}\right] + \frac{P_0^2}{PrRe}y + \frac{2(P_0+Re)P_0(\mathrm{e}^{Rey}-1)}{Re(1-Pr)(\mathrm{e}^{Re}-1)} - \frac{(P_0+Re)^2(\mathrm{e}^{2Rey}-1)}{2(2-Pr)(\mathrm{e}^{Re}-1)^2}\right\} \quad (11)$$

It is seen that the first terms in Eq. (11) is the solution of the energy equation when viscous dissipation is negligible and the second term results from viscous dissipation. As can be seen from Eq. (11) the temperature distribution is linearly dependent on the Eckert number. Furthermore, it is seen that as $Pr = 1$ and $Pr = 2$, the dimensionless temperature goes to infinity and this is not a realistic situation. For $Re = 0$ the solution of energy equation is also not valid from the same reason. Hence the solution of energy equation which is valid for $Pr = 1$ and $Pr = 2$ has to be obtained for the case of pressure-and-plate movement-driven flow. The general solution of energy equation valid for $Pr = 1$ can be obtained as follows:

$$\theta = A + B\mathrm{e}^{Rey} + \frac{EcP_0^2}{Re^3}y + \frac{2Ec(P_0+Re)P_0}{Re^2(\mathrm{e}^{Re}-1)}y\mathrm{e}^{Rey} - \frac{Ec(P_0+Re)^2}{2Re^2(\mathrm{e}^{Re}-1)^2}\mathrm{e}^{2Rey} \quad (12)$$

where A and B are the integration constants that are determined subject to boundary conditions given by Eq. (5) as follows:

$$A = -\frac{1}{(\mathrm{e}^{Re}-1)}\left[1 - \frac{2EcP_0(P_0+Re)\mathrm{e}^{Re}}{Re^2(\mathrm{e}^{Re}-1)} + \frac{Ec(P_0+Re)^2(\mathrm{e}^{2Re}-1)}{2Re^2(\mathrm{e}^{Re}-1)^2} - \frac{EcP_0^2}{Re^3}\right] + \frac{Ec(P_0+Re)^2}{2Re^2(\mathrm{e}^{Re}-1)^2}$$

$$B = \frac{1}{(\mathrm{e}^{Re}-1)}\left[1 - \frac{2EcP_0(P_0+Re)\mathrm{e}^{Re}}{Re^2(\mathrm{e}^{Re}-1)} + \frac{Ec(P_0+Re)^2(\mathrm{e}^{2Re}-1)}{2Re^2(\mathrm{e}^{Re}-1)^2} - \frac{EcP_0^2}{Re^3}\right]$$

The solution of energy equation valid for $Pr = 1$ is obtained by substituting the integration constants into Eq. (12) as follows:

$$\theta = \frac{\mathrm{e}^{Rey}-1}{(\mathrm{e}^{Re}-1)} + \frac{Ec}{Re^2}\left\{\frac{\mathrm{e}^{Rey}-1}{(\mathrm{e}^{Re}-1)}\left[-\frac{2P_0(P_0+Re)\mathrm{e}^{Re}}{(\mathrm{e}^{Re}-1)} + \frac{(P_0+Re)^2(\mathrm{e}^{2Re}-1)}{2(\mathrm{e}^{Re}-1)^2} - \frac{P_0^2}{PrRe}\right] + \frac{P_0^2}{Re}y + \frac{2P_0(P_0+Re)}{(\mathrm{e}^{Re}-1)}y\mathrm{e}^{Rey} - \frac{(P_0+Re)^2(\mathrm{e}^{2Rey}-1)}{2(\mathrm{e}^{Re}-1)^2}\right\} \quad (13)$$

Similarly, for the pressure-and-plate movement-driven flow, the general solution of energy equation valid for $Pr = 2$ is found to be as follows:

$$\theta = A + B\mathrm{e}^{2Rey} + \frac{EcP_0^2}{Re^3}y - \frac{4Ec(P_0+Re)P_0}{Re^3(\mathrm{e}^{Re}-1)}\mathrm{e}^{Rey} - \frac{Ec(P_0+Re)^2}{Re(\mathrm{e}^{Re}-1)^2}y\mathrm{e}^{2Rey} \quad (14)$$

By applying the boundary conditions Eq. (5) the integration constants are determined to be

$$A = -\frac{1}{(\mathrm{e}^{2Re}-1)}\left[1 + \frac{4EcP_0(P_0+Re)}{Re^3} + \frac{Ec(P_0+Re)^2\mathrm{e}^{2Re}}{Re(\mathrm{e}^{Re}-1)^2} - \frac{EcP_0^2}{Re^3}\right] + \frac{4EcP_0(P_0+Re)}{Re^3(\mathrm{e}^{Re}-1)}$$

$$B = \frac{1}{(\mathrm{e}^{2Re}-1)}\left[1 + \frac{4EcP_0(P_0+Re)}{Re^3} + \frac{Ec(P_0+Re)^2\mathrm{e}^{2Re}}{Re(\mathrm{e}^{Re}-1)^2} - \frac{EcP_0^2}{Re^3}\right]$$

Combining Eq. (14) with the determined integration constants yields

$$\theta = \frac{\mathrm{e}^{2Rey}-1}{(\mathrm{e}^{2Re}-1)} + \frac{Ec}{Re}\left\{\frac{\mathrm{e}^{2Rey}-1}{(\mathrm{e}^{2Re}-1)}\left[\frac{4P_0(P_0+Re)}{Re^2} + \frac{(P_0+Re)^2\mathrm{e}^{2Re}}{(\mathrm{e}^{Re}-1)^2} - \frac{P_0^2}{Re^2}\right] + \frac{P_0^2}{Re^2}y - \frac{4P_0(P_0+Re)(\mathrm{e}^{Rey}-1)}{Re^2(\mathrm{e}^{Re}-1)} - \frac{(P_0+Re)^2}{(\mathrm{e}^{Re}-1)^2}y\mathrm{e}^{2Rey}\right\} \quad (15)$$

Eq. (7) for $Pr \neq 2$ and Eq. (8) for $Pr = 2$ will be used for evaluating the dimensionless temperature distributions for the case of the lower plate movement-driven flow in the two large parallel plates whose walls are porous and at different temperatures. Eq. (11) for $Pr \neq 1$ and $Pr \neq 2$ and Eq. (13) for $Pr = 1$ and Eq. (15) $Pr = 2$ will be used for evaluating the dimensionless temperature distributions for the case of the pressure-and-plate movement-driven flow in the two large parallel plates with porous walls that are at different values of temperatures.

After obtaining the temperature distributions for these cases, one can analyze irreversibility of the process by applying the second law of thermodynamics. The total entropy generation includes contributions due to heat conduction in both the transverse direction and viscous dissipation resulting from fluid friction. In other words, heat transfer processes are generally accompanied by thermodynamic irreversibility or entropy generation. The generation of entropy may be due to a variety sources, primarily heat transfer down temperature gradients, characteristic of convective heat transfer and viscous dissipation.

3. Entropy generation in an incompressible fluid confined in a slit

Consider an incompressible fluid is flowing in the x-direction in a horizontal thin slit whose walls are porous and at different temperature. It is assumed that laminar viscous flow through a thin slit subjected to constant wall temperature takes place for fluid possessing constant physical properties (ρ, μ, k, C_P). Thus, entropy generation is unavoidable due to conduction heat transfer through the fluid and viscous dissipation. If we consider a two-dimensional infinitesimal fluid element and consider the element as an open thermodynamic system subjected to mass fluxes, energy transfer and entropy transfer interactions through a fixed control surface, the volumetric rate of entropy generation for incompressible Newtonian fluid in Cartesian coordinates is given as follows [20]:

$$S_{\mathrm{G}} = \frac{k}{T^2}\left[\left(\frac{\partial T}{\partial \tilde{x}}\right)^2 + \left(\frac{\partial T}{\partial \tilde{y}}\right)^2\right] + \frac{\mu}{T}\left[\left(\frac{\partial \tilde{v}_x}{\partial \tilde{y}}\right)^2\right] \tag{16}$$

The above Eq. (16) indicates that the irreversibility or entropy generation results from the heat conduction in both transverse and axial directions and viscous dissipation.

The dimensionless entropy generation rate called the local entropy generation number [9] is obtained by dividing the total entropy generation rate equation (16) with the characteristic entropy transfer rate ($S_{\mathrm{G,C}}$) that is defined as

$$S_{\mathrm{G,C}} = \left[\frac{k(\Delta T)^2}{h^2 T_1^2}\right] \tag{17}$$

In the above equation, ΔT is the difference of temperatures between two plates (T_2–T_1), T_1 is the absolute reference temperature and h is the characteristic length that depends on geometry and type of problem. Here it is equal to the transverse distance between two large plates. The dimensionless entropy generation rate that is obtained by dividing the dimensionless form of Eq. (16) with Eq. (17) is given as follows (see [9]):

$$N_{\mathrm{S}} = \frac{1}{Pe^2}\left(\frac{\partial \theta}{\partial x}\right)^2 + \left(\frac{\partial \theta}{\partial y}\right)^2 + \frac{Br}{\Omega}\left[\left(\frac{\partial v_x}{\partial y}\right)^2\right] \tag{18}$$

$$Pe = \rho C_p u_{\mathrm{m}} h/k, \Omega = \Delta T/T_1 \quad \text{and} \quad Br = Pr \times Ec = \mu u_{\mathrm{m}}^2/(k\Delta T)$$

where Pe is the Peclet number, Br is the Brinkman number and Ω is the dimensionless temperature difference.

Eq. (18) can be expressed alternatively as follows:

$$N_{\mathrm{S}} = N_X + N_Y + N_{\mathrm{F}} \tag{19}$$

On the right hand side of Eq. (19) the first term (N_X) denotes the entropy generation by heat transfer due to the axial conduction, the second term (N_Y) accounts for the entropy generation by heat transfer due to the transverse conduction and the last term (N_{F}) represents the entropy generation due to viscous dissipation.

As mentioned earlier it was assumed that the flow is laminar and fully developed in the x-direction which requires that one-dimensional flow occurs in the axial direction and a temperature gradient in the transverse direction; therefore, Eq. (18) can be reduced to the following equation:

$$N_{\mathrm{S}} = \left(\frac{\partial \theta}{\partial y}\right)^2 + \frac{Br}{\Omega}\left[\left(\frac{\partial v_x}{\partial y}\right)^2\right] \tag{20}$$

For $Pr \neq 2$ the entropy generation number for the lower plate movement case is given by

$$N_{\mathrm{S}} = \left\{\frac{PrRe\mathrm{e}^{RePry}}{(\mathrm{e}^{RePr}-1)}\left[1 + \frac{EcPr(\mathrm{e}^{2Re}-1)}{2(2-Pr)(\mathrm{e}^{Re}-1)^2}\right] - \frac{2ReEcPr\mathrm{e}^{2Rey}}{2(2-Pr)(\mathrm{e}^{Re}-1)^2}\right\}^2 + \frac{PrEcRe^2}{\Omega(\mathrm{e}^{Re}-1)^2}\mathrm{e}^{2Rey} \tag{21}$$

and the similar equation for $Pr = 2$ is obtained as follows:

$$N_{\mathrm{S}} = \left\{\frac{2Re\mathrm{e}^{2Rey}}{(\mathrm{e}^{2Re}-1)}\left[1 + \frac{Ec\mathrm{e}^{2Re}}{2(\mathrm{e}^{Re}-1)^2}\right] - \frac{ReEc\mathrm{e}^{2Rey}}{2(\mathrm{e}^{Re}-1)^2} - \frac{Re^2Ec}{(\mathrm{e}^{Re}-1)^2}y\mathrm{e}^{Rey}\right\}^2 + \frac{2EcRe^2}{\Omega(\mathrm{e}^{Re}-1)^2}\mathrm{e}^{2Rey} \tag{22}$$

Eqs. (21) and (22) are obtained by substituting the derivatives of Eqs. (2a), (7) and (8) with respect to y into Eq. (18).

Similarly, for $Pr \neq 1$ and $Pr \neq 2$ the entropy generation number for the pressure gradient and plate movement case is given by

$$N_S = \left\{ \frac{PrRe e^{RePry}}{(e^{RePr}-1)} + \frac{EcPr}{Re^2} \times \left[\left(-\frac{2P_0(P_0+Re)}{Re(1-Pr)} + \frac{P_0(P_0+Re)^2(e^{2Re}-1)}{2(2-Pr)(e^{Re}-1)^2} - \frac{P_0^2}{RePr} \right) \times \frac{PrRe e^{RePry}}{(e^{RePr}-1)} + \frac{P_0^2}{RePr} + \frac{2P_0(P_0+Re)e^{Rey}}{Re(1-Pr)(e^{Re}-1)} - \frac{Re(P_0+Re)^2 e^{2Rey}}{(2-Pr)(e^{Re}-1)^2} \right]^2 + \frac{PrEc}{\Omega} \left(\frac{(P_0+Re)^2 e^{2Rey}}{(e^{Re}-1)^2} - \frac{2P_0(P_0+Re)e^{Rey}}{Re(e^{Re}-1)} + \left(\frac{P_0}{Re}\right)^2 \right) \right. \quad (23)$$

One obtains Eq. (23) by substituting the derivatives of Eqs. (2b) and (11) with respect to y into Eq. (20). The entropy generation equations valid for $Pr = 1$ and $Pr = 2$ are derived by inserting the derivatives of Eqs. (2b), (13) and (15) with respect to y into Eq. (20) and resulting equations for the pressure-and-plate movement-driven flow are given as follows: For $Pr = 1$

$$N_S = \left\{ \frac{Re e^{Rey}}{(e^{Re}-1)} + \frac{Ec}{Re^2} \times \left[\frac{Re e^{Rey}}{(e^{Re}-1)} \left(-\frac{2P_0(P_0+Re)e^{Re}}{(e^{Re}-1)} + \frac{(P_0+Re)^2(e^{2Re}-1)}{2(e^{Re}-1)^2} - \frac{P_0^2}{Re} \right) + \frac{P_0^2}{Re} + \frac{2P_0(P_0+Re)e^{Rey}}{(e^{Re}-1)} + \frac{2P_0Re(P_0+Re)}{(e^{Re}-1)} y e^{Rey} - \frac{Re(P_0+Re)^2 e^{2Rey}}{(e^{Re}-1)^2} \right]^2 + \frac{Ec}{\Omega} \left(\frac{(P_0+Re)^2 e^{2Rey}}{(e^{Re}-1)^2} - \frac{2P_0(P_0+Re)e^{Rey}}{Re(e^{Re}-1)} + \left(\frac{P_0}{Re}\right)^2 \right) \right. \quad (24)$$

For $Pr = 2$

$$N_S = \left\{ \frac{2Re e^{2Rey}}{(e^{2Re}-1)} + \frac{2Ec}{Re} \times \left[\frac{2Re e^{2Rey}}{(e^{2Re}-1)} \left(\frac{2P_0(P_0+Re)}{Re^2} + \frac{(P_0+Re)^2 e^{2Re}}{2(e^{Re}-1)^2} - \frac{P_0^2}{Re^2} \right) + \frac{P_0^2}{2Re^2} - \frac{2P_0(P_0+Re)e^{Rey}}{Re(e^{Re}-1)} - \frac{(P_0+Re)^2}{2(e^{Re}-1)^2} e^{2Rey} - \frac{Re(P_0+Re)^2}{(e^{Re}-1)^2} y e^{2Rey} \right]^2 + \frac{2Ec}{\Omega} \left(\frac{(P_0+Re)^2 e^{2Rey}}{(e^{Re}-1)^2} - \frac{2P_0(P_0+Re)e^{Rey}}{Re(e^{Re}-1)} + \left(\frac{P_0}{Re}\right)^2 \right) \right. \quad (25)$$

The equations obtained for entropy generation for both flow cases, namely the plate movement-driven flow and pressure-and-plate movement-driven flow, will be used for determining entropy generation profiles as functions of cross-flow Reynolds number, the Prandtl number, the Eckert number and the dimensionless temperature difference.

4. Results and discussion

The convective heat transfer processes are analyzed by the second law of thermodynamics namely entropy generation due to irreversibility of the processes. As stated earlier, there exists a direct proportionality between irreversibility, quantified in the entropy generated, and the amount of useful and available work lost in the process. In convective heat transfer both fluid frictions and heat transfer make contributions to the rate of entropy generation.

Although it is desirable to consider the Ec and Pr in a group that is called the Brinkman number ($Br = Ec \times Pr$) for evaluating the relative importance of the energy due to viscous dissipation to the energy because of heat conduction, in the present study the Brinkman number is not used for evaluating the obtained results since the Ec and Pr do not always appear together in the derived equations. It was reported that Br is much less than unity for many engineering processes [9]. The irreversibility distribution ratio is defined as the ratio of entropy generation due to fluid frictions (N_F) to heat transfer ($N_X + N_Y$). In other words, it is equal to the ratio of Brinkman number to the dimensionless temperature difference (Br/Ω). The irreversibility distribution ratio denoted by ϕ can be interpreted as; the case of $0 \leqslant \phi < 1$ indicates that heat transfer irreversibility dominates over fluid friction irreversibility and the fluid friction dominates over heat transfer irreversibility when $\phi > 1$. For the case of $\phi = 1$, both the heat transfer and fluid friction have the same contribution for entropy generation. An alternative irreversibility distribution parameter was defined by Paoletti et al. [21] as ratio of entropy generation due heat transfer to the total entropy generation that is called Bejan number given by

$$Be = \frac{N_X + N_Y}{N_S} = \frac{1}{1+\phi} \quad (26)$$

The above equation can be interpreted according to values of ϕ as described above. Hence, the range of Bejan number is between 0 and 1. The value of $Be = 1$ indicates that the heat transfer irreversibility dominates over fluid friction, which corresponds to the case of $\phi = 0$. On the other hand, a value of Be equal to zero indicates that the fluid friction irreversibility dominates over the irreversibility because of the heat transfer, which corresponds the limit of $\phi \to \infty$. The case of $Be = 1/2$ shows that the entropy generation due to heat transfer and fluid friction irreversibility are equal to one another, and corresponds to the case of $\phi = 1$. By substituting the derivative of Eqs. (7) and (21) into Eq. (26), Bejan number for $Pr \neq 2$ can be obtained for the lower plate movement-driven fluid flow as follows:

$$Be=\frac{\left\{\frac{PrRee^{RePry}}{(e^{RePr}-1)}\left[1+\frac{EcPr(e^{2Re}-1)}{2(2-Pr)(e^{Re}-1)^2}\right]-\frac{2ReEcPre^{2Rey}}{2(2-Pr)(e^{Re}-1)^2}\right\}^2}{\left[\left\{\frac{PrRee^{RePry}}{(e^{RePr}-1)}\left[1+\frac{EcPr(e^{2Re}-1)}{2(2-Pr)(e^{Re}-1)^2}\right]-\frac{2ReEcPre^{2Rey}}{2(2-Pr)(e^{Re}-1)^2}\right\}^2+\frac{PrEcRe^2}{\Omega(e^{Re}-1)^2}e^{2Rey}\right]} \tag{27}$$

Similarly, Be number for the pressure-and-upper plate movement-driven flow can be obtained as in Eq. (28) by substituting the derivative of Eqs. (11) and (23) into Eq. (26) for $Pr\neq 1$ and $Pr\neq 2$.

Be numbers for $Pr=1$ and $Pr=2$ can be also easily obtained in the same manner for the pressure-and-upper plate movement-driven flow; however, they will not be obtained in the present investigation. Bejan number for each flow case can be numerically computed as functions of the Prandtl number, the Reynolds number, the Eckert number and the dimensionless temperature difference from Eqs. (27) and (28) by using the specific numerical values other than 1.0 and 2.0 for Pr. Similarly, the entropy generation number as functions of Pr, Re, Ec and Ω for each flow case can be numerically computed from Eq. (21) for the plate movement-driven flow at values of $Pr\neq 2$ and from Eq. (23) for the pressure-and-plate movement-driven flow at values of $Pr\neq 1$ and $Pr\neq 2$.

The dimensionless steady state temperature profiles as a function of Prandtl number at different values of Reynolds number ($Re=-3.0$ and $Re=3.0$) for $Ec=0$ are depicted in Fig. 3 for a fluid subjected to lower plate movement and in Fig. 3 for a fluid subjected to a pressure drop and the upper plate movement. As can be seen from the figures the temperature profiles approach the plates with increasing the Prandtl number for two flow cases. While the temperature profiles become close to the lower plate for the case of mass suction, those become close to the upper plate for the case of transverse mass injection from the bottom wall. The figures indicate that the plates will be close to adiabatic wall with increasing Prandtl numbers. In other words, the plates will be close to adiabatic with increasing molecular diffusivity of momentum relative to molecular diffusivity of heat since Prandtl number measures the relative importance of momentum diffusivity to heat diffusivity.

in the solution of energy equation. It is seen that, if the viscous dissipation term is ignored in the energy equation, the temperature profile for the same magnitude of mass suction/injection will be symmetric in a Newtonian fluid between two large plates. As a result, the symmetric temperature profiles are obtained for both flow problems namely the plate movement-driven flow and the pressure-and-plate movement-driven flow in a thin slit when the viscous dissipation term is neglected. It is seen from comparison of Fig. 3 with Fig. 4 that the temperature profiles for the pressure-and-plate movement-driven flow become much closer to the lower plate than that for the plate movement-driven flow with increasing the mass suction at the bottom plate and enhances heat transfer at this plate. On the other hand, for the case of mass injection from bottom plate the pressure-and-plate movement-driven flow will reduce heat transfer at the bottom wall and enhance heat transfer at the upper one more than the plate movement-driven flow. As can be seen from Figs. 3 and 4 temperature profiles become much closer to the lower and upper plates for the pressure-and-plate movement-driven flow than that for the plate movement-driven flow alone. The velocity profiles for two flow cases also move toward either the upper plate or the lower plate depending on whether mass is injected or sucked at the bottom plate. Since the temperature profiles will be much closer to the plates with increasing the transverse mass suction/injection, it is expected that for very large mass injection/suction the plate will be close to adiabatic wall. However, when the Eckert number is not negligible, the viscous dissipation term in the solution of energy equation will make considerable contribution to heat generation in the fluid and thus, the temperature profiles will be different from those shown in Figs. 3 and 4. As mentioned previously, in order to take into account the viscous dissipation term in the energy equation the Eckert number will be non-zero. Therefore, the influence of the viscous dissipation on the temperature profile can be examined by varying values of the Eckert number. The effect of Eckert number on the temperature profile is illustrated in Figs. 3 and 4 at constant values of Prandtl number

$$Be=\frac{\left\{\frac{PrRee^{RePry}}{(e^{RePr}-1)}+\frac{EcPr}{Re^2}\left[\left(-\frac{2P_0(P_0+Re)}{Re(1-Pr)}+\frac{P_0(P_0+Re)^2(e^{2Re}-1)}{2(2-Pr)(e^{Re}-1)^2}-\frac{P_0^2}{RePr}\right)\times\frac{PrRee^{RePry}}{(e^{RePr}-1)}+\frac{P_0^2}{RePr}+\frac{2P_0(P_0+Re)e^{Rey}}{Re(1-Pr)(e^{Re}-1)}-\frac{Re(P_0+Re)^2e^{2Rey}}{(2-Pr)(e^{Re}-1)^2}\right]\right\}^2}{\left\{\frac{PrRee^{RePry}}{(e^{RePr}-1)}+\frac{EcPr}{Re^2}\left[\left(-\frac{2P_0(P_0+Re)}{Re(1-Pr)}+\frac{P_0(P_0+Re)^2(e^{2Re}-1)}{2(2-Pr)(e^{Re}-1)^2}-\frac{P_0^2}{RePr}\right)\times\frac{PrRee^{RePry}}{(e^{RePr}-1)}+\frac{P_0^2}{RePr}+\frac{2P_0(P_0+Re)e^{Rey}}{Re(1-Pr)(e^{Re}-1)}-\frac{Re(P_0+Re)^2e^{2Rey}}{(2-Pr)(e^{Re}-1)^2}\right]\right\}^2+\frac{PrEc}{\Omega}\left(\frac{(P_0+Re)^2e^{2Rey}}{(e^{Re}-1)^2}-\frac{2P_0(P_0+Re)e^{Rey}}{Re(e^{Re}-1}+\left(\frac{P_0}{Re}\right)^2\right)} \tag{28}$$

As stated previously the first terms in Eqs. (7), (8), (11), (13) and (15) are the solutions of energy equations valid for specific values of Prandtl number when the viscous dissipation term is negligible. Therefore, the solution of energy equation is arranged such that the taking Eckert number equal to zero means neglecting the viscous dissipation term

($Pr=1.0$) and dimensionless temperature difference ($\Omega=1.0$) for the cases of mass suction ($Re=-3.0$) and injection ($Re=3.0$). As can be seen from the figures the fluid temperature increase to be higher than that of plate with increasing the Eckert number for the both fluid flow cases. Since there is a linear relationship between the

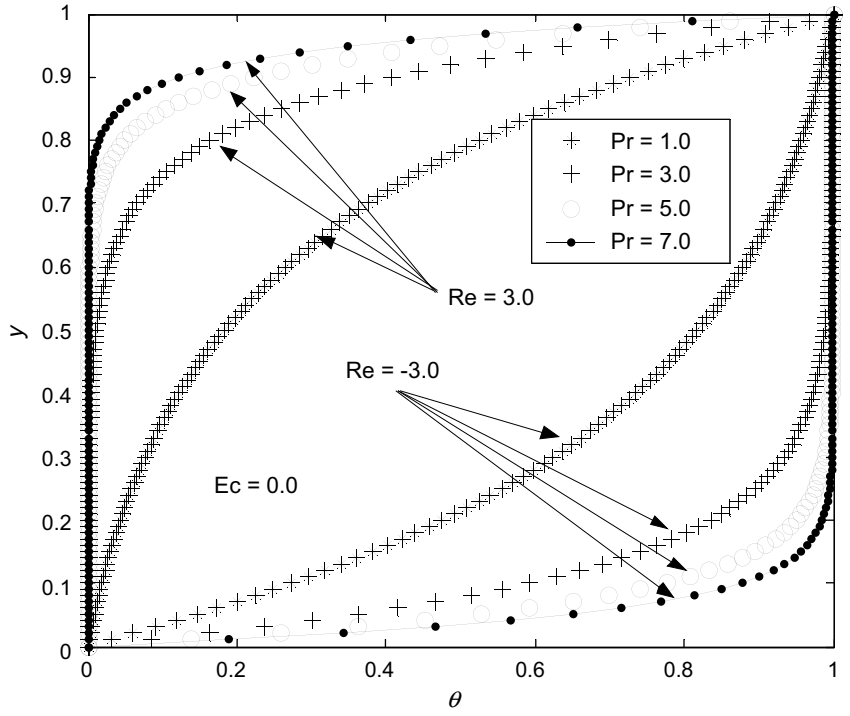

Fig. 3. Temperature variations with the Prandtl number for the plate movement-driven flow.

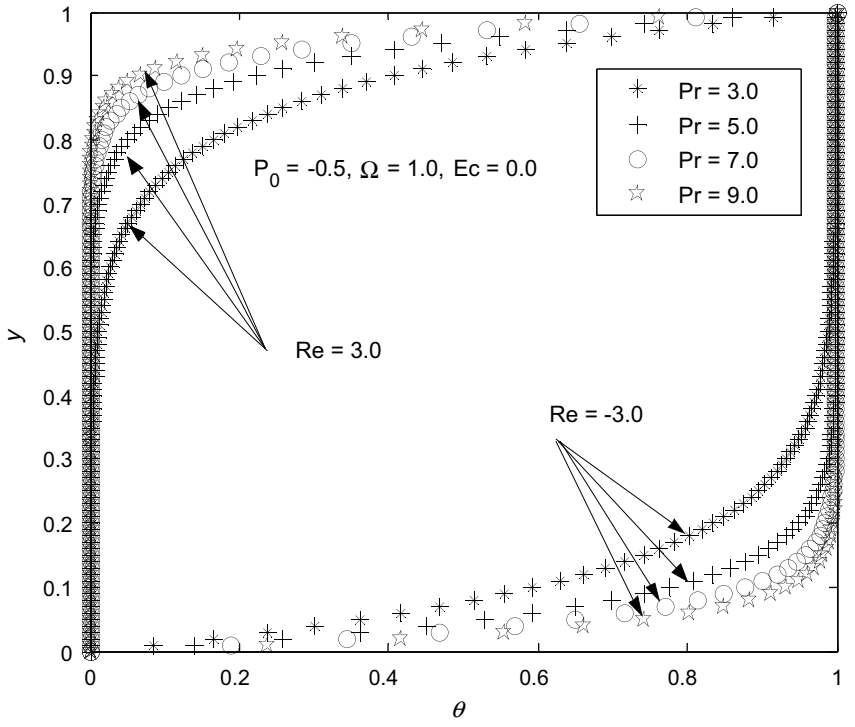

Fig. 4. Temperature variations with the Prandtl number for the pressure-and-plate movement-driven flow.

irreversibility distribution ratio and the Eckert number, an increase in the Eckert number will result in the same amount of increase in the irreversibility distribution ratio at constant values of Prandtl number and dimensionless temperature difference. Therefore, the irreversibility increases with increasing the Eckert number, which results in increasing fluid temperature due to heat generation because of fluid friction.

It is also seen that the temperature profile of the fluid as a function of the Eckert number for mass suction and injec-

tion are substantially different from one another at the same magnitude of the other effective parameters. As stated previously the magnitudes of mass suction and injection has a large influence on the temperature profile of the fluid. Fig. 5 shows that while the fluid temperature is lower than the upper plate temperature for mass injection/suction cases at value of $Ec = 1.0$, the fluid temperature increases to be higher than the upper plate temperature with increasing Eckert number due to viscous dissipation. On the other hand, Fig. 6 indicates that the fluid temperature is lower than the upper plate temperature for mass injection and slightly higher than that for mass suction at the value of $Ec = 1.0$ for constant values of the dimensionless pressure drop ($P_0 = -0.5$), the dimensionless temperature difference

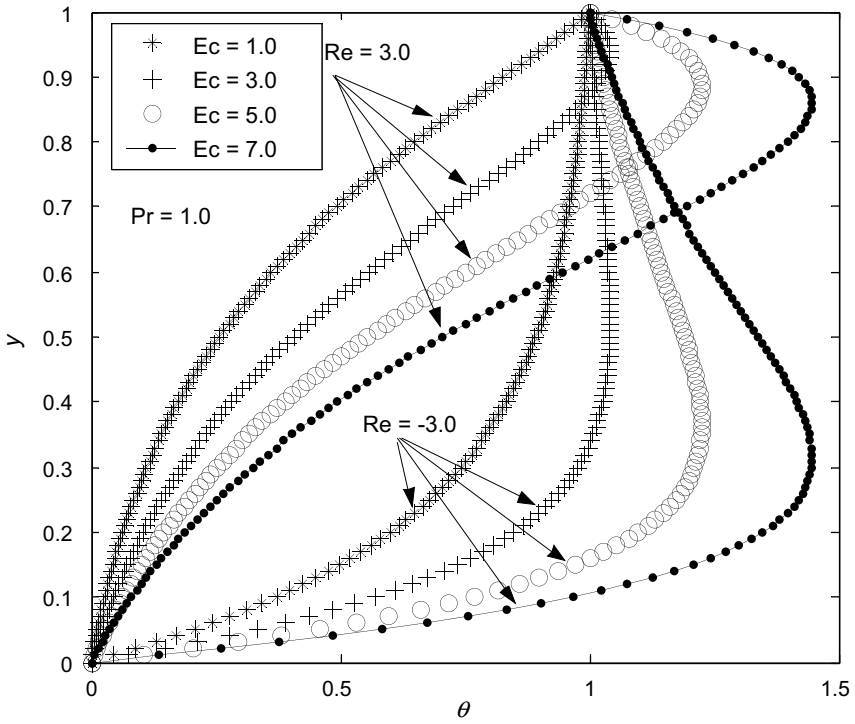

Fig. 5. Temperature variations with the Eckert number for the plate movement-driven flow.

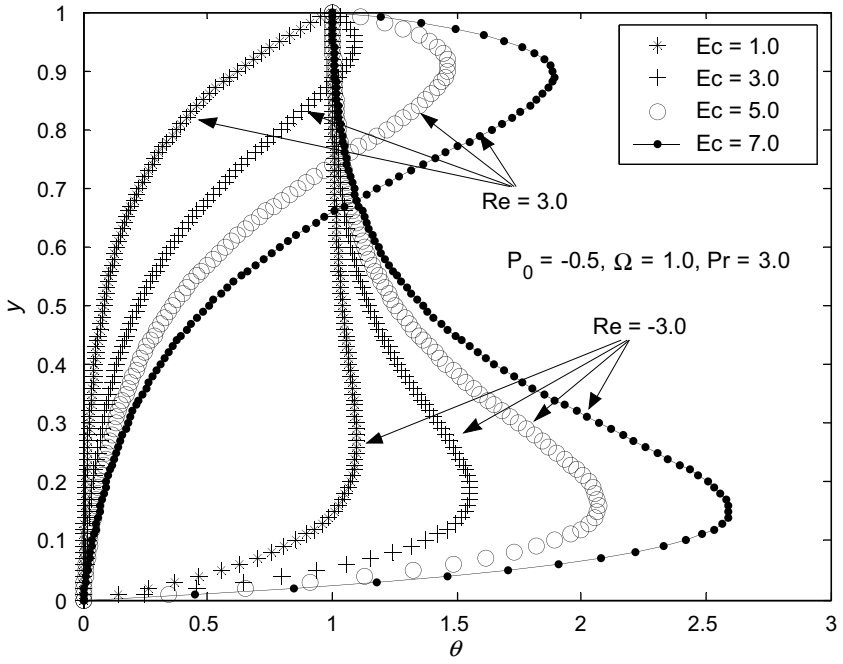

Fig. 6. Temperature variations with the Eckert number for the pressure-and-plate movement-driven flow.

($\Omega = 1.0$) and Prandtl number ($Pr = 3.0$). It is also observed that the fluid temperature profiles for the pressure-and-plate movement-driven flow are affected by the Eckert number more than that for the plate movement-driven flow for both mass suction and injection cases (compare Figs. 5 and 6 with one another). Furthermore, the fluid temperature for the pressure-and-plate movement-driven flow increases more rapidly than that for the plate movement fluid with increasing the Eckert number and there is a maximum increase in the fluid temperature at each values of the Eckert number for both flow cases and for both the transverse mass transfer cases (mass suction and injection) at constant values of Pr, Ω, and P_0. It is also observed from the figure that the magnitudes of the fluid temperature for the mass suction case is larger than that of the fluid temperature for the mass injection case. Although the trend observed for the fluid temperature profiles in the pressure-and-plate movement-driven flow is similar to those in the plate movement-driven flow, their magnitudes are quite different. In other words, the magnitudes of the fluid temperature for the pressure-and-plate movement-driven flow are larger than those of the fluid temperature for the plate movement-driven flow. Thus, it can be said that the viscous dissipation effect on the fluid temperature for the pressure-and-plate movement-driven flow is more pronounced than that for the plate movement-driven flow. Eqs. (7), (8), (11), (13) and (15) are the solutions of energy equations which were obtained for certain values of Prandtl numbers. The second and third terms on the right hand side of these equations come from the viscous dissipation. As can be seen Ec number in those equations lies as a multiplier of viscous dissipation terms. Therefore, an increase in Ec number will directly reflect to the increase in dimensionless temperature of the fluid as pointed out in Figs. 5 and 6. As can be seen in Fig. 6 when Ec number increases to be 7.0, the dimensionless temperature of the fluid becomes much higher than that of the upper plate especially for the pressure-and-plate movement-driven fluid flow. The large amount of increase in the dimensionless temperature may arise a question that whether the chosen values of the dimensionless quantities violate the accepted assumptions such as laminar flow and incompressibility. Unfortunately we do not have experimental data for the chosen values of the dimensionless quantities to evaluate system for deciding whether violation takes place or not. Although it is not shown here, the effect of the Prandtl number at the constant values of the Eckert number, the dimensionless temperature difference and the pressure drop are examined for the both flow cases at varying values of Reynolds number ($Re = -3.0$ and $Re = 3.0$). It is observed that the fluid temperature increases to be higher than that of plate temperature with increasing Prandtl number larger than 1. This trend is observed for both flow cases; however, as mentioned previously the magnitudes of the fluid temperature for the pressure-and-plate movement-driven flow are more pronounced than that for the plate movement-driven fluid flow. The value of the maximum fluid temperature occurring close to the lower plate for the mass suction is much higher than that occurring close to the upper plate for

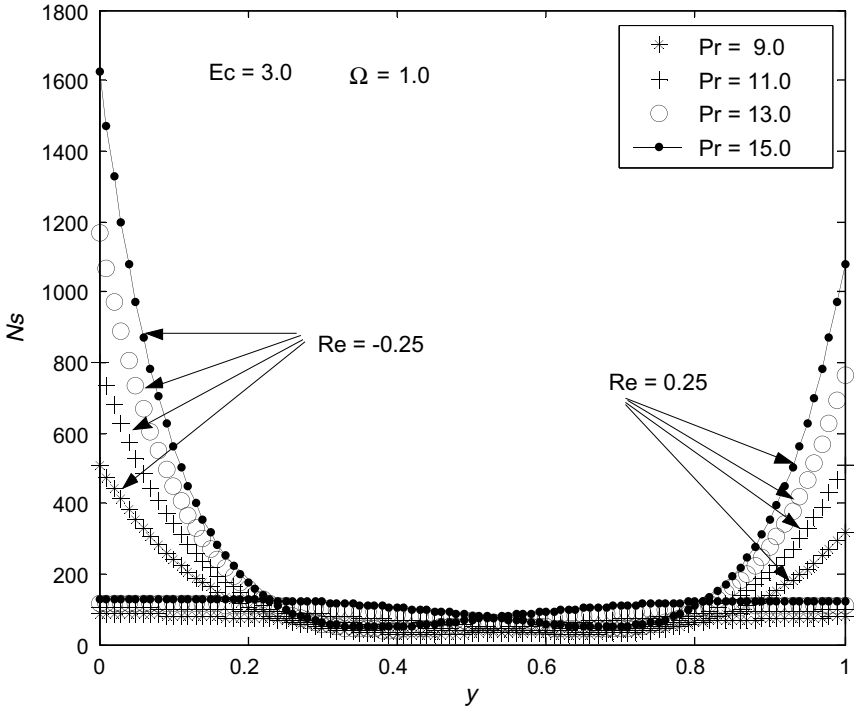

Fig. 7. Effect of the Prandtl number on the entropy generation for the plate movement-driven flow.

the mass injection at the bottom plate. Therefore, it can be concluded that the mass suction influence on the fluid temperature is more effective than mass injection.

Note that Prandtl number and Eckert number affect the fluid temperature in a similar way. As expressed earlier Pr, Ec and Ω can be written altogether to give a group called as irreversibility distribution ratio ($\phi = PrEc/\Omega$); however, in the present study the effect of only ϕ instead of Pr and Ec on the fluid temperature and entropy distributions is not examined since these parameters usually do not appear together in the solution of energy equations for both flow cases.

The dimensionless entropy generation number (N_S) as a function of Prandtl number at $Ec = 3.0$ and $\Omega = 1.0$ for the plate movement-driven flow and the pressure-and-plate movement-driven flow is, respectively, shown in Figs. 7 and 8 for varying values of Reynolds number (mass suction/injection). As can be seen from Fig. 7 the maximum entropy generation takes place at the lower plate for the mass suction and at the upper plate for the mass injection. While Fig. 7 is drawn for the plate movement-driven fluid flow, Fig. 8 is depicted for the pressure-and-plate movement-driven fluid flow. Although magnitude of the dimensionless entropy generation is different from one another for both flow cases, the trend observed for the entropy generation in the plate movement-driven fluid flow is similar to that in the pressure-and-plate movement-driven fluid flow. For the plate movement-driven fluid flow the entropy generation takes a value of around 500 on the bottom plate while for the pressure-and-plate movement-driven flow it takes a value of 680 on the bottom plate at the same magnitudes of Pr, Ec, Ω and Re. As can be seen from both figures entropy generations on the plates increase with increasing Prandtl number. Therefore, it can be said that molecular diffusivity of momentum become more important than that of heat at, or near, the plates. Although it is not clearly seen from Fig. 7 there is a lowest value for entropy generation in the fluid flowing between two large plates. The location in which the lowest entropy generation occurs is significantly dependent on either the mass suction or the mass injection and slightly dependent on the Prandtl number. For the pressure-and-plate movement-driven flow, while the lowest entropy generation occurs at a value of $y = 0.38$ for the case of the mass suction, that takes place at a value of $y = 0.68$ for the case of mass injection at constant values of the pressure drop ($P_0 = -0.50$), the dimensionless temperature difference ($\Omega = 1.0$) and the Eckert number ($Ec = 3.0$). The observation for entropy generation indicates that there is a close relationship between entropy generation profile and velocity profile, i.e., the velocity profile maximum corresponds to the place where the entropy generation profile attains a minimum value. In addition, the entropy generation increases with increasing the Prandtl number for both flow cases as seen in Figs. 7 and 8. In other words, the maximum entropy generation rate shifts to each plate as viscous effects becomes more important (i.e., as Pr increase). As expected the wall regions act as strong producers of irreversibility and thus entropy since

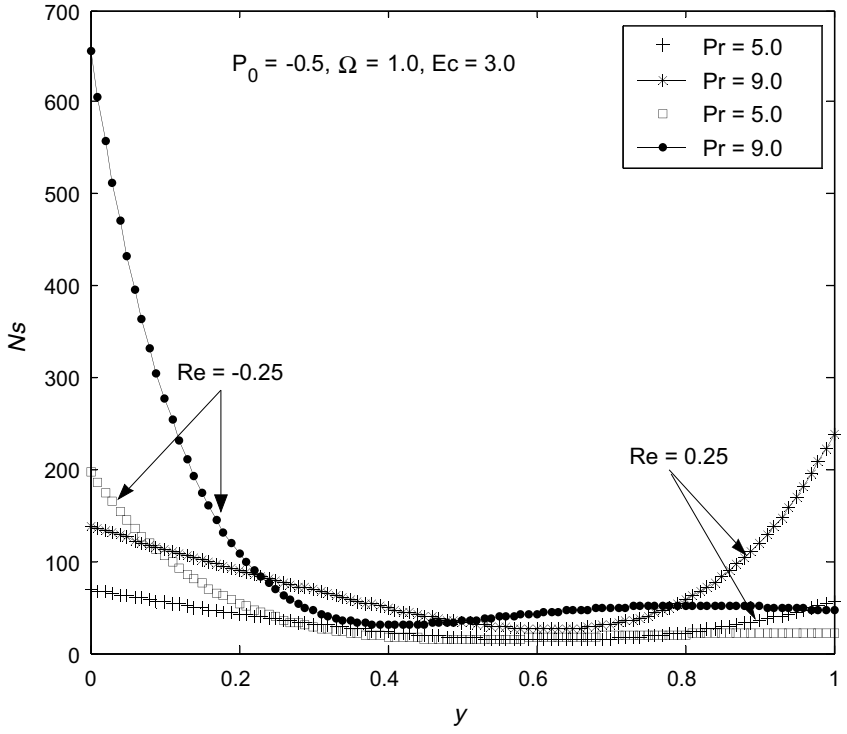

Fig. 8. Effect of the Prandtl number on the entropy generation for the pressure-and-plate movement-driven flow.

the viscous shear stress on the wall is maximum. The entropy generation on the lower plate for the case of the mass suction is higher than that on the upper plate for the case of mass injection at the same magnitudes of Reynolds number. As can be seen from Fig. 8 the entropy generation changes to be almost constant by decreasing the Prandtl number, which corresponds to a constant temperature in the fluid between two plates.

In order to examine the effect of the dimensionless temperature difference (Ω) on the entropy generation, Fig. 9 is depicted for the entropy generation as a function of the dimensionless temperature difference at the constant value of the Prandtl number ($Pr = 9.0$) and the Eckert number ($Ec = 3.0$) for the plate movement-driven flow. As can be seen from the figure the entropy generation is slightly dependent on the dimensionless temperature difference (Ω) for both the mass suction and mass injection at $Pr = 9.0$ and $Ec = 3.0$. The maximum entropy generation occurs on the plates since the maximum irreversibility is generated on the walls. For the mass suction at the bottom plate the entropy generation occurring on the lower plate is higher than that occurring on the upper plate for the mass injection. It can also be seen from the figure there is the lowest entropy generation in the fluid depending on the mass suction/injection at the bottom plate. The trend observed for the entropy generation as a function of the Ω is similar to that observed for the entropy generation as a function of the Prandtl number.

For the pressure-and-plate movement-driven flow the entropy generation as a function of dimensionless temperature difference is sketched in Fig. 10 at the constant values of the pressure drop ($P_0 = -0.50$), the Eckert number ($Ec = 3.0$) and the Prandtl number ($Pr = 5.0$) under only the mass injection. As can be seen from the figure all profiles for entropy generation other than that for $\Omega = 1.0$ are almost identical. Therefore, it can be said that the effect of dimensionless temperature on the entropy generation is negligible. It can also be said that the entropy generation slightly decreases with increasing dimensionless temperature.

Until this point the influence of effective parameters on the temperature and the entropy generation profiles is examined for two values of Reynolds number specifically the mass suction and the mass injection at the bottom wall.

The entropy generation as a function of the Reynolds number is drawn in Fig. 11 at the constant values of the Eckert number ($Ec = 8.0$), the Prandtl number ($Pr = 5.0$) and the dimensionless temperature difference ($\Omega = 1.0$) for the fluid that is flowed by the plate movement. As stated previously, the maximum entropy takes place either at the upper plate or at the lower plate according to the mass injection and mass suction. As can be seen from the figure the entropy generation on the plates increases with increasing the magnitudes of Reynolds number since the irreversibility due to fluid friction increases with increasing Reynolds number. In addition, there is a lowest value for the entropy generation in the fluid for both mass suction and injection although the location varies according to the magnitude and sign of Reynolds number. Furthermore, the largest value for the entropy generation on the lower plate is obtained for the largest mass suction. On the other hand, the highest value for the entropy generation on the upper plate is obtained for the largest mass injection from

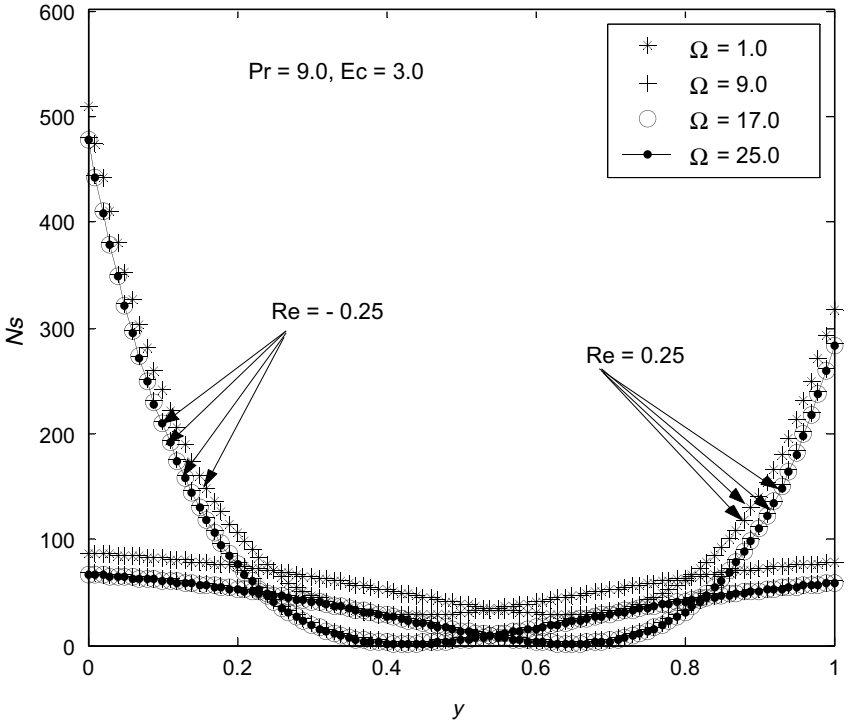

Fig. 9. Effect of the dimensionless temperature difference on the entropy generation for the plate movement-driven flow.

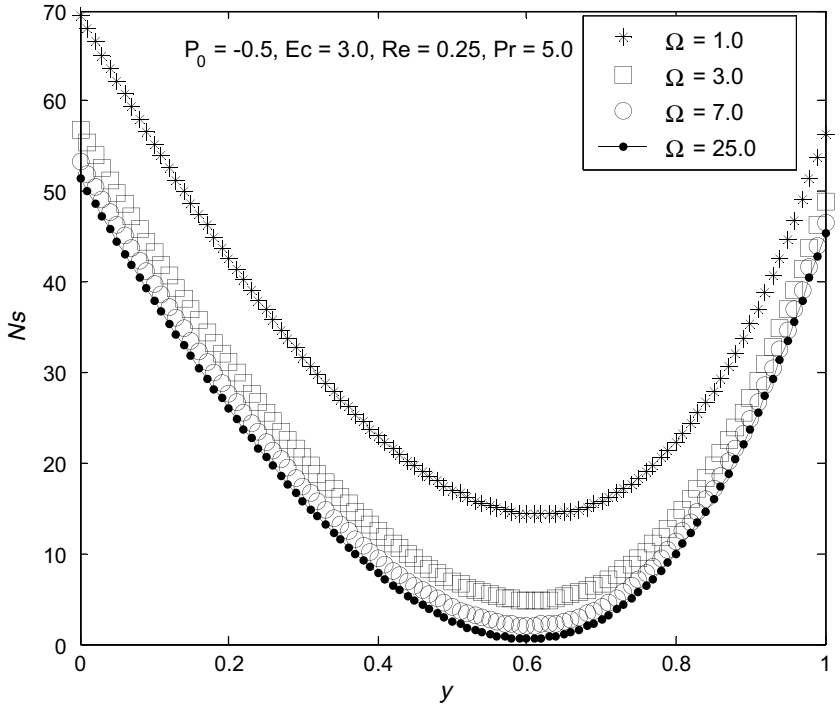

Fig. 10. Effect of the dimensionless temperature difference on the entropy generation for the pressure-and-plate movement-driven flow for the case of only mass injection.

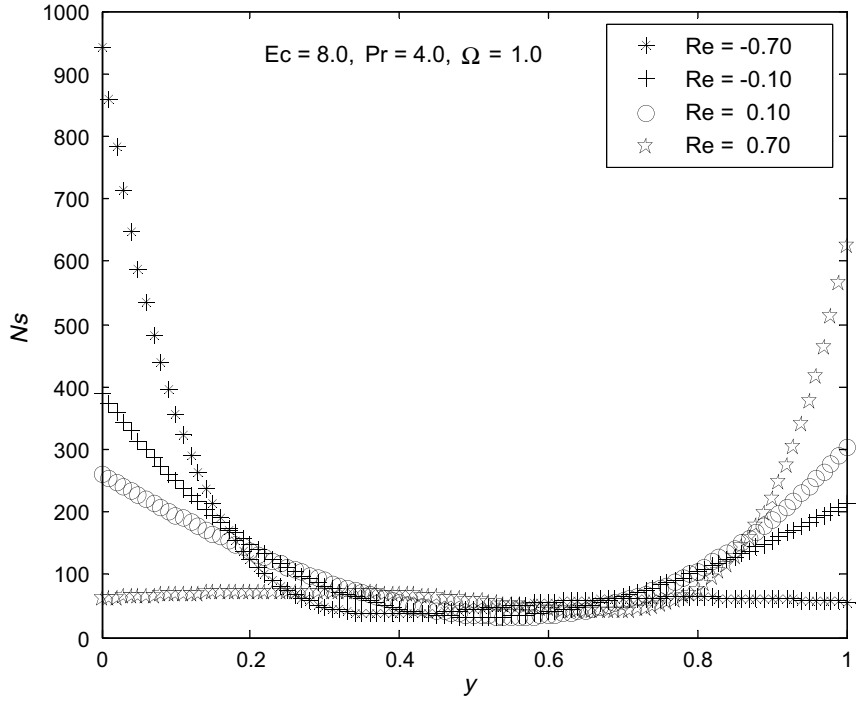

Fig. 11. Effect of the Reynolds number on the entropy generation for the plate movement-driven flow.

the bottom plate. Therefore, it can be concluded that an increase in the momentum transfer from the plates to the fluid will enhance the entropy generation in boundary layer since the velocity profile of the fluid between two large plates moves close to the lower plate by the mass suction and moves close to the upper plate by the mass injection. The entropy generation occurring at a location close to the lower plate is higher than that occurring at a location close to the upper plate at the large magnitudes of Reynolds number.

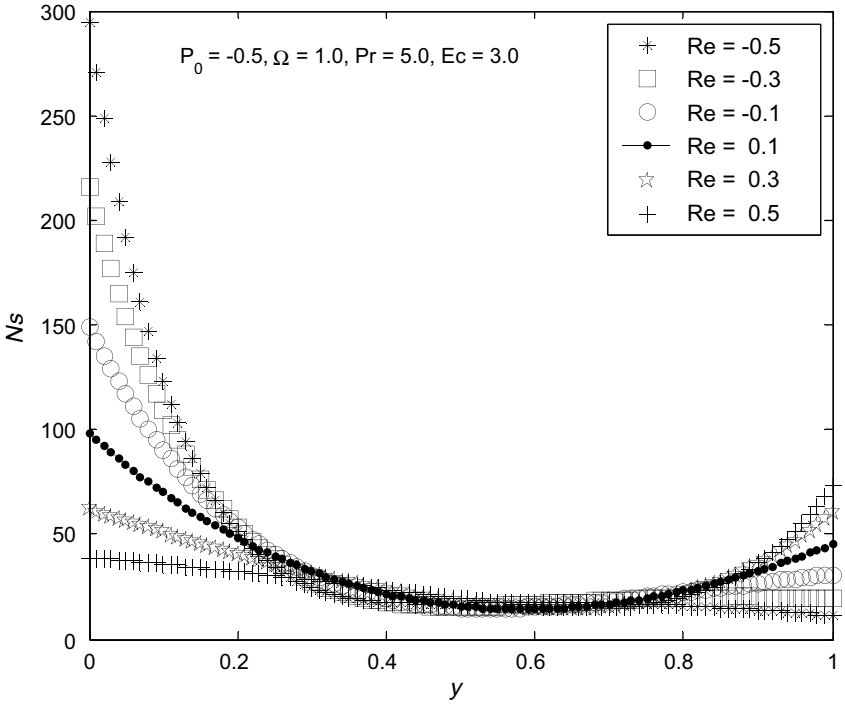

Fig. 12. Effect of the Reynolds number on the entropy generation for the pressure-and-plate movement-driven flow.

For the pressure-and-plate movement-driven fluid flow, the entropy generation as a function of the cross-flow Reynolds number is illustrated in Fig. 12 at the constant values of the pressure drop ($P_0 = -0.50$), the Eckert number ($Ec = 3.0$), the Prandtl number ($Pr = 5.0$) and the dimensionless temperature difference ($\Omega = 1.0$). As can be seen from the figure the entropy generation increases with increasing amount of the mass suction/injection. The increase of the entropy generation for the case of mass suction is more pronounced than that for the case of mass injection with increasing magnitudes of Reynolds number when other parameters are kept constant at the same values.

As a result, the trend observed here for the entropy generation as functions of the Prandtl number, the Eckert number, the dimensionless temperature difference and the cross-flow Reynolds number is similar to that observed by Bejan [9], Sahin [13] and Mahmud and Fraser [14] for the entropy generation of a Newtonian fluid flow in various cross-sectional geometries.

The observations made in the present study can be extended to the flow past moving vehicles, pylons of bridges and buildings. Fransson et al. [23] reported that suction delays separation contributing to a narrower wake width, and a corresponding reduction of drag force, whereas blowing indicates the opposite behavior. In other words, the drag force on the body decreases drastically with increasing suction rate. Furthermore, porous walls have been used in many instruments such as compact diffusers, fuel cells, some of heat exchangers, wind tunnels, combustion chambers etc. For instance, a porous-wall compact diffuser can be designed for chemical layer applications and by improving the earliest ventilated wind tunnels porous walls have been started to use in such instruments. Therefore, the present study can be extended to examine entropy generations in those instruments.

5. Conclusion

The second law analysis of laminar viscous flow of the fluid in a thin horizontal slit whose plates at different temperatures has been performed to determine the dimensionless temperature and total entropy generation distributions as functions of the Prandtl number, the Eckert number, the dimensionless temperature difference for the cases of mass suction and injection. The temperature and entropy generation profiles have been interpreted in terms of the effective parameters such as Pr, Ec, Ω and Re. It is concluded that the plates becomes close to adiabatic wall with increasing Prandtl number at $Ec = 0$. Furthermore, it is observed that for the case of mass injection from bottom plate, the pressure-and-plate movement-driven flow will reduce heat transfer at the bottom wall and enhance heat transfer at the upper plate more than the plate movement-driven flow. The slit wall regions act as strong irreversibility producers since viscous shear stress near the wall attains its maximum value. It is also observed that the temperature profile of the fluid as a function of the Eckert number for the cases of mass suction and injection are substantially different from one another at the same magnitude of the other effective parameters. The magnitudes of mass suction and injection have a large influence on the temperature profile of the fluid. It is also observed that Prandtl number and Eckert number affect the fluid temperature in the similar way.

The maximum entropy generation rate shifts to each plate as viscous effects becomes more important since the wall regions act as strong irreversibility producers due to more fluid frictions in wall regions. It is found that an increase in values of the cross-flow Reynolds number (mass suction/injection) enhances the entropy generation in boundary layer since the velocity profile of the fluid between two large plates moves close to the lower plate for the mass suction and moves close to the upper plate for the mass injection. The entropy generation is slightly dependent on the dimensionless temperature difference (Ω) for both the mass suction and mass injection at certain values of Pr and Ec.

References

[1] J. Wang, Z. Gao, G. Gan, D. Wu, Analytical solution of flow coefficients for a uniformly distributed porous channel, Chem. Eng. Sci. 84 (2001) 1–6.

[2] T. Hayat, A.H. Kara, E. Mononiat, Exact flow of a third-grade fluid on a porous wall, Int. J. Non-linear Mech. 38 (2003) 1533–1537.

[3] T. Fang, A note on the incompressible Couette flow with porous walls, Int. Commun. Heat Mass Transfer. 31 (1) (2004) 31–41.

[4] T. Fang, Further discussion on the incompressible pressure-driven flow in a channel with porous walls, Int. Commun. Heat Mass Transfer 31 (4) (2004) 487–500.

[5] C. Deng, D.M. Martinez, Viscous flow in a channel partially filled with a porous medium and with wall suction, Chem. Eng. Sci. 60 (2005) 329–336.

[6] P.D. Ariel, On exact solutions of flow problems of a second grade fluid through two parallel porous walls, Int. J. Eng. Sci. 40 (2002) 913–941.

[7] M.B. Zaturska, W.H.H. Banks, New solution for flow in a channel with porous walls and/or non-rigid walls, Fluid Dyn. Res. 33 (2003) 57–71.

[8] A. Ogulu, E. Amos, Asymptotic approximations for the flow field in a free convective flow of a non-Newtonian fluid past a vertical porous plate, Int. Commun. Heat Mass Transfer 32 (2005) 974–982.

[9] A. Bejan, A study of entropy generation in fundamental convective heat transfer, J. Heat Transfer 101 (1979) 718–725.

[10] P.K. Nag, P. Mukherjee, Thermodynamic optimization of convective heat transfer through a duct with constant wall temperature, Int. J. Heat Mass Transfer 30 (1987) 401–405.

[11] S.H. Tasnim, S. Mahmud, Entropy generation in a vertical concentric channel with temperature dependent viscosity, Int. Commun. Heat Mass Transfer 29 (2002) 907–918.

[12] A.Z. Sahin, Second law analysis of laminar viscous flow through a duct subjected to constant wall temperature, J. Heat Transfer 120 (1998) 76–83.

[13] A.Z. Sahin, A second law comparison for optimum shape of duct subjected to constant wall temperature and laminar flow, Heat Mass Transfer 33 (1998) 425–430.

[14] S. Mahmud, R.A. Fraser, The second law analysis in fundamental convective heat transfer problems, Int. J. Therm. Sci. 42 (2003) 177–186.

[15] S. Mahmud, R.A. Fraser, Second law analysis of forced convection in a circular duct for non-Newtonian fluids, Energy 31 (2006) 2226–2244.

[16] P. Naphon, Second law analysis on the heat transfer of the horizontal concentric tube heat exchanger, Int. Commun. Heat Mass Transfer 33 (2006) 1029–1041.

[17] Z.Y. Guo, S.Q. Zhou, Z.X. Li, L.G. Chen, Theoretical analysis in fundamental convective heat transfer problems, Int. J. Heat Mass Transfer 45 (2002) 2119–2127.

[18] F. Kamisli, Laminar flow of a non-Newtonian fluid in channels with wall suction or injection, Int. J. Eng. Sci. 44 (2006) 650–661.

[19] F. Kamisli, Pressure-driven laminar flow of a non-Newtonian fluid in a slit with wall suction or injection, Chem. Eng. Proc., in press, corrected proof, Available online 3 December 2006.

[20] A. Bejan, Entropy Generation through Heat and Fluid Flow, Wiley, New York, 1982.

[21] S. Paoletti, F. Rispoli, E. Sciubba, Calculation exergetic loses in compact heat exchanger passages, ASME AES 10 (1989) 21–29.

[22] F.M. White, Viscous Fluid Flow, McGraw-Hill, New York, 1974.

[23] J.H.M. Fransson, P. Konieczny, P.H. Alfredsson, Flow around a porous cylinder subject to continuous suction or blowing, J. Fluids Struct. (19) (2004) 1031–1048.